JBC RESEARCH ARTICLE

Elucidation of the interaction proteome of mitochondrial chaperone Hsp78 highlights its role in protein aggregation during heat stress

Received for publication, February 4, 2022, and in revised form, September 1, 2022 Published, Papers in Press, September 15, 2022,
https://doi.org/10.1016/j.jbc.2022.102494

Witold Jaworek[1], **Marc Sylvester**[2], **Giovanna Cenini**[1], **and Wolfgang Voos**[1,*]

From the [1]*Institute of Biochemistry and Molecular Biology (IBMB), Faculty of Medicine, University of Bonn, Bonn, Germany;* [2]*Core Facility Mass Spectrometry, Institute of Biochemistry and Molecular Biology (IBMB), University of Bonn, Faculty of Medicine, Bonn, Germany*

Edited by Ursula Jakob

Chaperones of the Hsp100/Clp family represent major components of protein homeostasis, conferring maintenance of protein activity under stress. The ClpB-type members of the family, present in bacteria, fungi, and plants, are able to resolubilize aggregated proteins. The mitochondrial member of the ClpB family in *Saccharomyces cerevisiae* is Hsp78. Although Hsp78 has been shown to contribute to proteostasis in elevated temperatures, the biochemical mechanisms underlying this mitochondria-specific thermotolerance are still largely unclear. To identify endogenous chaperone substrate proteins, here, we generated an Hsp78-ATPase mutant with stabilized substrate-binding behavior. We used two stable isotope labeling–based quantitative mass spectrometry approaches to analyze the role of Hsp78 during heat stress–induced mitochondrial protein aggregation and disaggregation on a proteomic level. We first identified the endogenous substrate spectrum of the Hsp78 chaperone, comprising a wide variety of proteins related to metabolic functions including energy production and protein synthesis, as well as other chaperones, indicating its crucial functions in mitochondrial stress resistance. We then compared these interaction data with aggregation and disaggregation processes in mitochondria under heat stress, which revealed specific aggregation-prone protein populations and demonstrated the direct quantitative impact of Hsp78 on stress-dependent protein solubility under different conditions. We conclude that Hsp78, together with its cofactors, represents a recovery system that protects major mitochondrial metabolic functions during heat stress as well as restores protein biogenesis capacity after the return to normal conditions.

Every organism requires specific biochemical processes for the maintenance of the internal protein homeostasis, keeping cellular functions intact and the cell alive. Due to the exposition to variable environmental conditions, especially immobile organisms like bacteria, fungi, and plants suffer from thermal stress and therefore exhibit distinct protective mechanisms that convey a certain degree of thermotolerance. Also human cells may be subjected to heat stress under certain pathological conditions like fever. These proteo-protective mechanisms are based on the activity of molecular chaperones, representing ATP-dependent enzymes that stabilize misfolded proteins, protecting them from aggregation and support degradation processes (1–4). One important group of chaperones with a major role during protein aggregation reactions is the Hsp100 chaperone family. They belong to the AAA+ class of enzymes (ATPase associated with wide variety of cellular activities), many of them involved in molecular remodeling reactions (5). Enzymes of a particular subgroup of the Hsp100 family, all relatives of the bacterial ClpB protein, are able to resolve polypeptides from insoluble aggregates and to support their refolding *via* the Hsp70 chaperone system or their degradation through various ATP-dependent proteases (6, 7). ClpB-type chaperones typically form hexameric ring structures that are formed by intermolecular interactions of their two AAA protein domains. It was proposed that the mechanistic basis of the chaperone activity is based on a threading mechanism of the polypeptide chains through the central pore of the ring complex, thereby dissolving any incorrect protein conformations (3). Bacterial ClpB was shown to cause thermal hypersensitivity in the respective null-mutant strains, thus ClpB-type chaperones facilitate thermal tolerance to bacteria (8). In comparison to other Hsp100 chaperones, ClpB-type proteins do not directly assemble with proteases (9).

The problematic nature of heat stress might be even more relevant for mitochondrial proteins as it is assumed that, due to metabolic processes, temperature inside the organelle may be elevated permanently (10). The basic biochemical mechanisms of the chaperone enzymes involved in mitochondrial aggregation have been largely established to date, either based on the utilization of artificial reporter proteins or the characterization of the thermal reactivity of single examples of specific proteins. However, for a complete understanding of mitochondrial protein homeostasis under thermal stress conditions, it is fundamental to identify proteins that exhibit less

* For correspondence: Wolfgang Voos, wolfgang.voos@uni-bonn.de.
Present address for Giovanna Cenini: Institute of Reconstructive Neurobiology, University of Bonn Medical Faculty & University Hospital Bonn, Venusberg-Campus 1, D-53127 Bonn, Germany

stable folding states and have a tendency to aggregate. Previous experiments exposing human cells to mild heat stress, similar to fever conditions, exhibited an overall quite robust behavior of mitochondrial proteins with only few polypeptides prone to aggregation (11). In contrast, a study in yeast established a strong effect of elevated temperatures on mitochondrial morphology (12). Yeast cells contain two homologs of bacterial Hsp100 family chaperone ClpB, the cytosolic Hsp104 (13), and the mitochondrial Hsp78 (14). As ClpB family members are not present in higher eukaryotes (15), it has been proposed that other chaperones, in particular mtHsp70 together with its cochaperone Tid1, may take over Hsp100 function in human mitochondria (16). Similar to other Hsp100 family members, Hsp78 is an ATP-dependent enzyme, which is upregulated upon thermal stress and most likely forms the typical barrel-shaped hexameric enzyme complexes with a central pore (17, 18). In analogy to bacterial ClpB, it is assumed also for Hsp78 that substrate polypeptides are mechanically pulled through the pore and are thereby disaggregated for further processes executed by other chaperone systems (19). Similar to other members of the family, Hsp78 contains two AAA-type nucleotide-binding domains with conserved Walker A and Walker B motifs (20), which are connected by a coiled-coil middle segment (M domain) that is proposed to provide an interaction with Hsp70-type chaperones, stimulating ATPase function (21). Due to its organellar localization, Hsp78 contains an N-terminal mitochondrial targeting sequence but lacks the N-terminal substrate-binding domain of bacterial ClpB (17). It is assumed that the N-terminal domain of ClpB plays a role in disaggregation of large aggregates (22), while there is little known about the mechanism of substrate interaction in case of the mitochondrial version.

Knowledge about the proteome stability inside mitochondria and the client pattern of the Hsp78 chaperone would provide fundamental information for the understanding of pathological patterns related to mitochondrial stress. So far, although some information is available on a whole-cell level (23), no comprehensive proteomic study was done in yeast mitochondria with the focus on Hsp78 disaggregation activity after heat stress. In our new study, we constructed a mutant form of Hsp78 with both AAA domains mutated in their Walker B motifs ($Hsp78_{TR}$). We aimed on generating a stabilized client–chaperone interaction due to an impaired capability to hydrolyze ATP. A similar approach was pursued for bacterial ClpB to identify endogenous substrate proteins (24). We performed a basic biochemical characterization of the mutant enzyme in order to check characteristics like complex formation and ATPase activity, as well as its general protein disaggregation competence. We focused on the identification of Hsp78-interacting proteins under normal and stress conditions, utilizing a quantitative proteomics approach. In a second quantitative mass spectroscopy (qMS) experiment, we demonstrate differences in protein aggregation and aggregate recovery between WT and mutant Hsp78 inside mitochondria on a proteomic level. The analysis revealed that Hsp78 plays a critical role in mitochondrial protein homeostasis with a focus on the reactivation of essential mitochondrial functions like TCA cycle and the respiratory chain but also including protein synthesis and import, after thermal stress exposure.

Results

$Hsp78_{TR}$ shows altered ATPase turnover but functional complex formation

We generated an Hsp78 ATPase-deficient mutant protein with both glutamic acids in the Walker B motifs exchanged to glutamine (E216Q/E614Q). Based on observation with a similar mutant form of the bacterial ClpB (24), we expected that the Hsp78 mutant would exhibit a higher substrate affinity to support the determination of the endogenous polypeptide client spectrum. The E216Q/E614Q mutant protein is abbreviated in the following as $Hsp78_{TR}$. In order to facilitate protein purification, we added a C-terminal 6× polyhistidine-tag (Fig. 1*A*). To serve as control for the biochemical properties of the mutant protein, a similar WT version was also generated. Both constructs were inserted in a yeast expression plasmid that allowed expression of the protein in a galactose-inducible fashion to avoid a long-term adaptation to the mutant phenotype. Proteins were expressed in a deletion background lacking the endogenous Hsp78 (*hsp78Δ*) so only the properties of the expressed proteins were analyzed. To check whether protein levels of WT and mutant proteins were comparable, we performed expression tests with both tagged proteins compared to an untagged WT version (Fig. 1*B*). Mutant $Hsp78_{TR}$ was expressed slightly weaker than the corresponding WT version although the His-tag had no severe effect on the expression level (Fig. 1*B*). ATPase activities of the Hsp78 variants were measured using purified protein expressed in *Escherichia coli* by a coupled enzymatic assay. The assay revealed a strong ATPase impairment of 70% in the $Hsp78_{TR}$ mutant compared to WT (Fig. 1*C*). Furthermore, a thermotolerance growth assay on nonfermentable carbon source (glycerol) was performed to analyze mitochondrial functionality after heat pretreatment at 42 °C for 60 min and a subsequent thermal shock at an otherwise lethal temperature of 48 °C for 60 min. Under these thermal stress conditions, the dependence of mitochondrial activity on the function of Hsp78 was clearly visible, showing a higher thermal resistance for cells expressing WT protein than mutant $Hsp78_{TR}$. In contrast, growth on fermentable carbon source (glucose) was similar (Fig. 1*D*).

In order to test complex formation of the expressed mutant Hsp78 under near-native conditions, we performed a blue-native (BN) PAGE with isolated mitochondria expressing the tagged constructs as described above. The majority of the Hsp78 signals were detected at sizes corresponding to a trimeric and hexameric complex, typical for ClpB-type chaperones. In particular with the trap mutant, we additionally detected a small amount of even higher molecular mass signals under ATP regenerating conditions (Fig. 1*E*, lane 2) that might represent chaperone complexes with bound polypeptide substrates. Moreover, we analyzed the purified proteins by size-exclusion chromatography showing formation of similar complexes with additional smaller and even higher complexes.

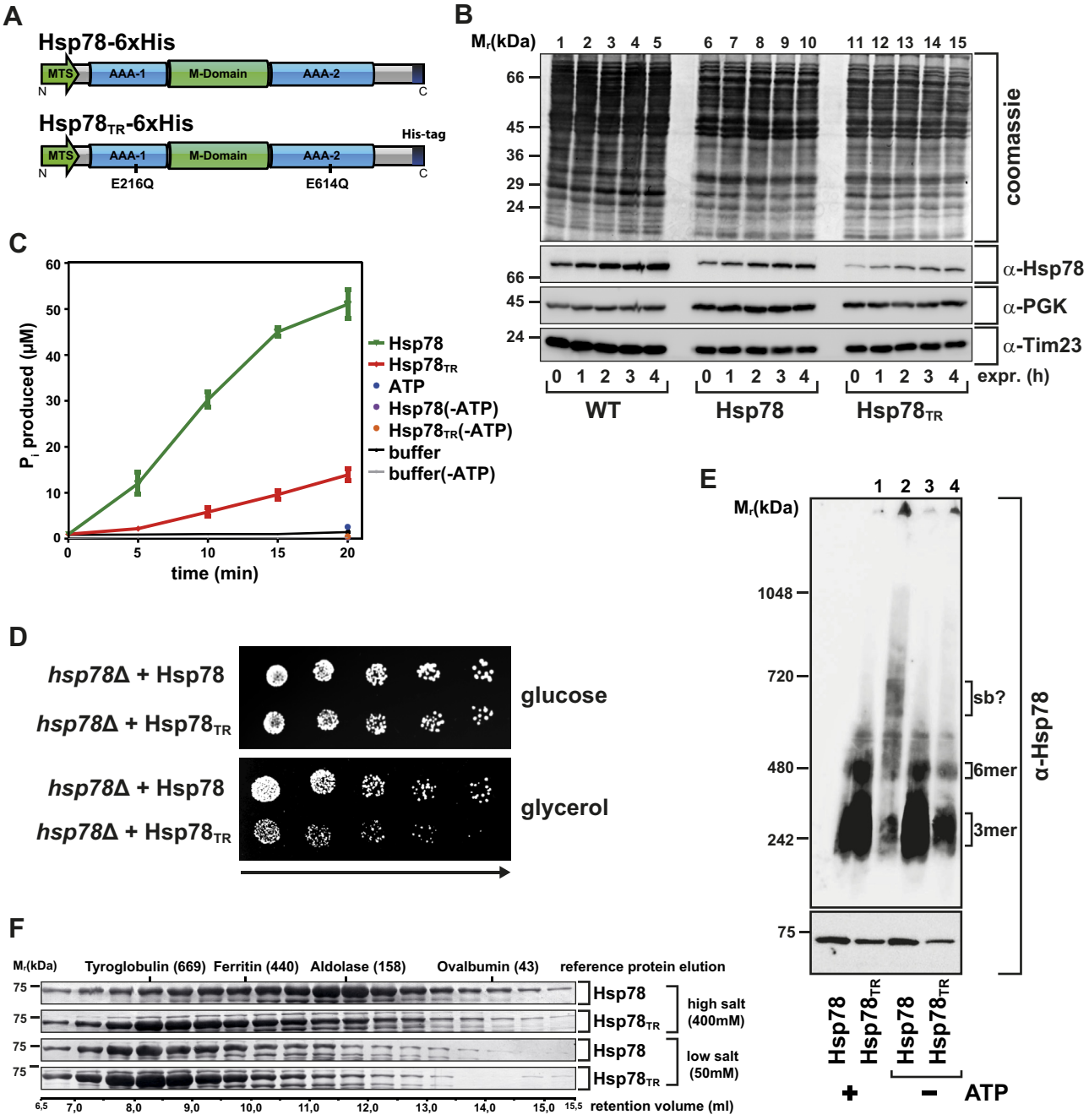

Figure 1. Hsp78 Walker B mutations impair ATPase activity and lead to altered protein behavior. *A*, schematic depiction of the WT (Hsp78) and mutant ($Hsp78_{TR}$) protein tagged with six histidine residues used in this study. In the mutant, both AAA-domains are modified in the Walker B section by amino acid exchange from glutamic acid to glutamine. *B*, yeast *hsp78Δ* cells expressing nontagged Hsp78 or the tagged Hsp78/$Hsp78_{TR}$ proteins were induced by addition of 2% galactose for the indicated time points, and protein levels were detected by SDS-PAGE and Western blot using α-Hsp78 antiserum. Decoration with α-Tim23 for control of mitochondrial content and α-PGK for general loading was performed. The upper panel shows the blot membrane stained with Coomassie Blue. *C*, ATPase activity determination of Hsp78 (*green curve*), $Hsp78_{TR}$ (*red curve*), and control reactions as indicated. Proteins were expressed and purified from *Escherichia coli*. Shown are mean values of three experiments; error bars indicate SEM. *D*, serial dilution growth test for acquired thermotolerance of *hsp78Δ* cells expressing either Hsp78 or $Hsp78_{TR}$ with 1:3 dilution steps. Cells were either plated on glucose (control) or on glycerol-containing plates and grown for at least 48 h at 30 °C. *E*, BN-PAGE (upper panel) and control SDS-PAGE (lower panel) with corresponding Western blots decorated with α-Hsp78 using mitochondria isolated from of *hsp78Δ* cells expressing either Hsp78 or $Hsp78_{TR}$. Mitochondria were resuspended either in resuspension buffer (+ATP) or in inhibition buffer (-ATP) prior to lysis. Indicated are the typical oligomeric forms of the chaperone (sb?, potential substrate-bound forms). *F*, sepharose-based gelfiltration size-exclusion chromatography with Hsp78 and $Hsp78_{TR}$ expressed and purified from *E. coli*. Fraction samples (0.5 ml each) were loaded on 12.5% SDS-PAGE and subsequent Coomassie Blue staining was performed. Protein samples were preincubated in high or low salt buffer as indicated. Retention volume indicates protein complex size by comparison with known high molecular proteins and complexes as reference. BN, blue native.

We also investigated complex stability by its resistance to high salt treatment. We found $hsp78_{TR}$ being stable up to concentrations of 400 mM NaCl in the buffer, while WT protein was dissociating into smaller oligomers (dimers and trimers) (Fig. 1*F*). We concluded that a higher complex stability for the mutant likely reflected a stronger client-binding capacity.

Taken together, we could show that our Hsp78 mutant is basically functional but exhibited a reduced ATPase activity and a stabilized complex formation.

Hsp78 is the key mitochondrial disaggregase and binds actively to aggregated proteins

Furthermore, we tested the influence of the novel Hsp78 mutant proteins on the mitochondrial disaggregation reaction. As an aggregation reporter, we utilized the fusion protein $b_2(107)\Delta$-$DHFR_{DS}$ that contains a thermo-labile dihydrofolate reductase domain with a matrix-targeting mitochondrial presequence (25). This reporter protein was imported in radioactively labeled form into isolated mitochondria, and aggregation was triggered by applying a short heat stress treatment. Afterward, the resolubilization of the reporter was determined by a comparison of the radioactive signal intensities in pellet and soluble fractions. Experiments were conducted for isolated WT mitochondria in presence or absence of ATP (Fig. 2*A*) or with *hsp78Δ* mitochondria overexpressing either Hsp78 or $Hsp78_{TR}$ (Fig. 2*B*). Quantification of the resolubilization efficiencies (Fig. 2*C*) showed a strongly reduced recovery activity for $Hsp78_{TR}$ with comparable values to knockout or WT control mitochondria without ATP supply. This shows that the inability of the mutant to hydrolyze ATP has a direct effect on its potential to resolubilize aggregated polypeptides.

To elucidate client interaction behavior of the $Hsp78_{TR}$ protein in comparison to the WT protein, we performed an aggregate-binding assay (experimental outline see Fig. 2*D*). First, a mix of aggregated mitochondrial polypeptides, serving as potential Hsp78-clients, was produced by a high-temperature treatment of *hsp78Δ* mitochondria, lysis, and subsequent high-velocity centrifugation obtaining an aggregate pellet (AP) without interference by Hsp78. Second, we generated cleared lysates of Hsp78 and $Hsp78_{TR}$-expressing mitochondria (S) that were not subjected to any heat treatment as chaperone sources. Next, the mitochondrial lysates containing the Hsp78 variants were incubated with the previously obtained resuspended AP to monitor potential client-binding reactions. Lysates and aggregated proteins were incubated together for 30 min at 30 °C and then centrifuged again. The chaperone detected in the pellet of the second centrifugation therefore reflected the amount bound to aggregated polypeptides. As control for a potential intrinsic aggregation propensity of the mutant $Hsp78_{TR}$, also the pellets (P) of mitochondrial lysates without any heat treatment were analyzed showing that only a minor amount of the mutated $Hsp78_{TR}$ was sedimented, most likely because the mutations introduced a certain instability of the polypeptide structure. Although the expression of Hsp78 in the cleared lysates was higher than that of $Hsp78_{TR}$, the experiment showed that $Hsp78_{TR}$ did cosediment stronger with the heat-induced aggregates than Hsp78 (P.AP+S lanes, Fig. 2*E*). The equally treated control samples in the absence of aggregate did not show any Hsp78 signal in the pellet fractions (P.C) (Fig. 2*E*), indicating that there was no unspecific aggregation of soluble chaperone species that could lead to false positive results. Taken together, the results indicate that Hsp78 is indeed interacting with aggregated polypeptides and that $Hsp78_{TR}$ mutant has a stronger substrate affinity than the WT protein, consistent with the expected effect of the mutagenesis.

Copurification studies reveal a variety of interacting mitochondrial proteins

In order to perform an unbiased identification of potential client proteins of Hsp78 in a natural organellar environment, we used Hsp78 and mutant $Hsp78_{TR}$ as overexpressed bait proteins in an affinity-based copurification procedure. Three different yeast strains expressing untagged Hsp78 as control, 6xHis-tagged Hsp78 and $Hsp78_{TR}$ mutant were cultured in minimal medium containing light, medium, and heavy nitrogen isotope amino acids, respectively. After isolation of mitochondria, organelles were lysed under native conditions and the Ni-metal affinity purification was performed (Fig. S1*A*). Samples of the copurification experiments confirmed a successful purification of the Hsp78 proteins, while the outer membrane protein Tom40, serving as internal control for an abundant noninteracting protein, showed no copurification (Fig. S1*B*), indicating the specificity of our approach. The eluates containing the different Hsp78 forms as well as copurifying polypeptides were combined (Fig. S1*C*) and subjected to stable isotope labeling by amino acids in culture (SILAC)-based quantitative mass spectrometry. Proteins identified in the untagged Hsp78 control sample were defined as background. These background abundance values were subtracted from the corresponding signal in the samples containing the respective tagged Hsp78 form as bait to allow a positive identification of potential interacting proteins.

In total, 465 proteins were at least once identified by MS in the different copurification experiments (raw qMS abundance values summarized in Table S2) of which 208 proteins exhibited a positive value above background. To correct for the differences in bait (Hsp78) expression levels, the interaction values were normalized to the qMS abundance of the respective Hsp78 variant (Table S3). To assess the specificity of the approach, we sorted all positively identified proteins according to their assigned cellular localization and plotted them based on their relative abundance values (Fig. 3*A*). Except for the Hsp78 samples at 25 °C, the cofractioned proteins were predominantly mitochondrial, indicating the validity of the approach. In most samples, more than 90% of the cofractionating protein amount were mitochondrial, with the majority located in the matrix compartment, as expected. The comparably large amount of nonmitochondrial proteins cofractioning with Hsp78 at 25 °C (about 45% of the total) likely indicated a high probability of nonspecific interactions that occur after lysis of mitochondria. In this sample, 41% of the total protein amount was represented solely by the proteins Lsp1 and Pil1, both very abundant proteins and components of the eisosome complex that is associated with the cell membrane. Hence, we suggest that these were purification artefacts. Another outlier protein was the mitochondrial outer membrane protein Om45

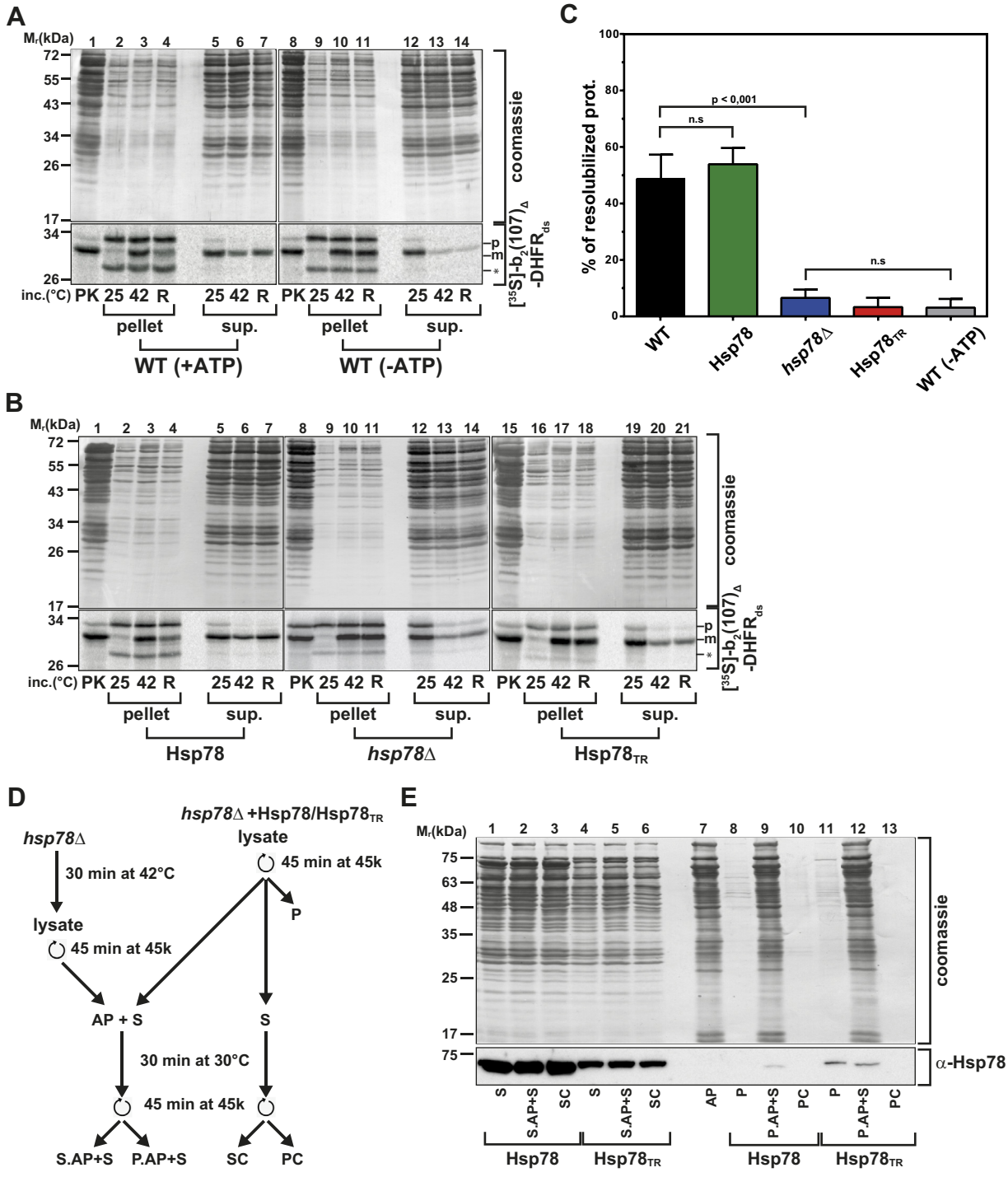

Figure 2. Hsp78 supports active disaggregation of heat-induced mitochondrial protein aggregates. *A*, disaggregation of imported reporter protein. [^{35}S]-labeled $b_2(107)_\Delta$-DHFR$_{ds}$ was imported for 20 min at 25 °C into isolated WT mitochondria. Mitochondria were then resuspended in presence (+ATP) or absence of ATP (-ATP), kept at 25 °C or stressed for 5 min at 42 °C. After recovery at 25 °C for 60 min (R), lysis and ultracentrifugation was performed for all samples. Supernatants and pellet fractions were collected and analyzed by SDS-PAGE. Nonimported preproteins were digested by protease K (PK) as indicated (preprotein, p; mature form, m). Asterisk (*) indicates additional translation product. As loading control, the Coomassie Blue–stained blot membrane is shown. *B*, import was performed as in (*A*) into *hsp78Δ* mitochondria overexpressing the indicated tagged proteins. Samples were resuspended in presence of ATP and analyzed as in (*A*). *C*, quantification of aggregation and recovery experiments from (*A*) and (*B*). Shown are bar diagrams with SEM and significance (n=5–7; n = 2 (-ATP); n. s., nonsignificant). *D*, flow scheme of aggregate-binding assay shown in (*E*). Aggregate pellets (AP) were prepared by lysis and centrifugation of heat-treated *hsp78Δ* mitochondria and combined with supernatant (S) fractions from untreated mitochondria expressing the indicated Hsp78 variants (AP+S). After incubation, aggregate-binding proteins were recovered by centrifugation (supernatant, S.AP+S; pellet, P.AP+S). Control reactions only contained supernatants (SC) and pellets (PC) without presence of aggregates. Indicated are heat treatments and centrifugation conditions. *E*, interaction of Hsp78 variants with aggregated proteins. Incubation of an AP derived from *hsp78Δ* mitochondria with the high speed centrifugation supernatants from mitochondria overexpressing tagged Hsp78 or Hsp78$_{TR}$ (as described in *D*) followed by SDS-PAGE, Western blot, and decoration with α-Hsp78 (Coomassie Blue staining as loading control).

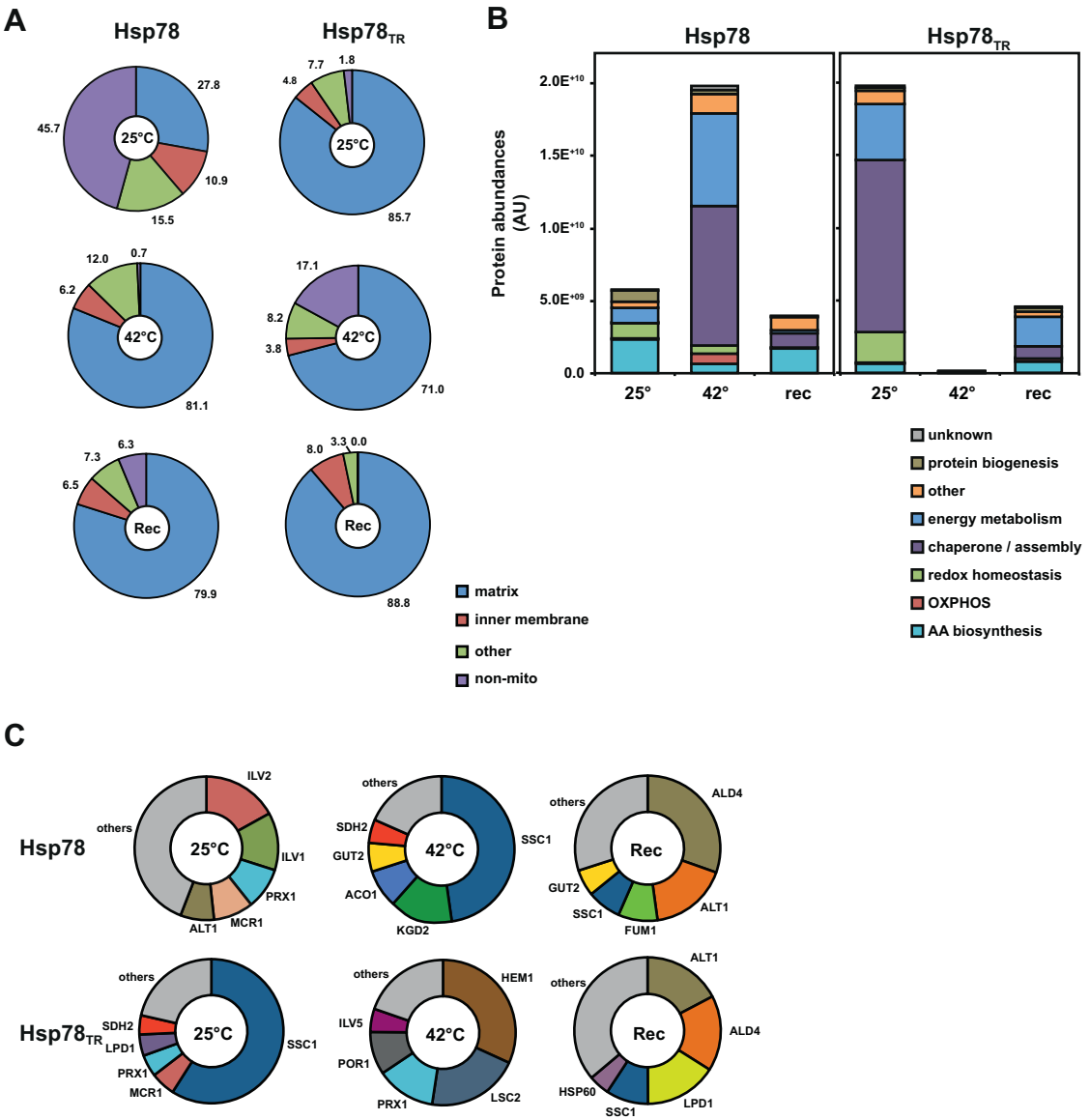

Figure 3. Hsp78 interaction proteome analysis by affinity-tag co-purification. *A*, subcellular localization distribution of proteins copurifying with Hsp78 and Hsp78$_{TR}$ after the indicated three temperature treatments. Protein hits were categorized by UNIPROT annotations. Protein qMS abundances were calculated as normalized average abundance over background from three independent experiments (see Experimental procedures section; data taken from Table S3). Relative values for abundance sums for the indicated cellular locations are shown (total sum of all protein abundances was set to 100%). *B*, abundance sums for WT and mutant copurification results sorted by the indicated functional categories. Only mitochondrial proteins are shown. OM45 has been omitted as a likely artefact. *C*, relative ratio of the five most abundant proteins found under the different conditions with both Hsp78 variants. qMS, quantitative mass spectroscopy.

that was found in all samples in very high amounts, representing at least 25% up to more than 80% of the cofractionating protein amounts. As Om45 is an integral membrane protein of the outer membrane with its bulk part exposed to the cytosol, it is very unlikely that it represents a potential Hsp78 client and was therefore excluded in the subsequent analysis of the quantitative data. In case of the WT form, the proportion of nonmitochondrial proteins decreased strongly during and after the 42 °C heat shock treatment, indicating that under stress conditions, the interaction specificity switched to the real endogenous client polypeptides. Interestingly, the overall binding behavior of the Hsp78$_{TR}$ mutant at 25 °C closely reflected that of the WT form under heat stress. This behavior likely correlates with the expected increased substrate-binding affinity of Hsp78$_{TR}$ already in absence of stress conditions. We also detected some inner membrane proteins binding to both Hsp78 forms with total ratio between 4% and 8%. This suggests that also some inner membrane proteins, likely that are exposed to the matrix compartment, can serve as potential Hsp78 clients. In addition, the specific effects of the different heat treatments already indicate a broad role of Hsp78 concerning mitochondrial thermal tolerance.

In order to assess the relevance of Hsp78 protein interaction for the function of mitochondrial proteins, we assigned the identified Hsp78-interacting mitochondrial proteins to their respective functional categories and sorted them by their signal

abundances, reflecting the absolute amounts of Hsp78-bound polypeptides (Fig. 3*B*). Concerning the total abundance sum of all interacting proteins, we observed a strong increase of protein binding for Hsp78 at 42 °C, supporting the hypothesis that Hsp78 is mainly functional under heat stress conditions. During the recovery period, the amount of bound proteins decreased significantly, suggesting that many client proteins are released from the chaperone after the heat stress has subsided. However, the pattern of functional categories bound during the recovery was different from that under normal conditions, indicating that certain client proteins undergo a prolonged interaction with the chaperone. The most abundant Hsp78-interacting proteins at 42 °C mainly fit into the categories 'chaperones/protein assembly' and 'energy metabolism' (mainly TCA cycle components), while the proteins from the categories 'redox homeostasis', 'OXPOS', and 'amino acid (AA) biosynthesis' were less strongly represented. In comparison, the mutant $Hsp78_{TR}$ showed the highest amount of interacting polypeptides already at 25 °C and almost no binding affinity under stress conditions, indicating the effect of the putative substrate-trap mutation and correlating with a functional defect at elevated temperatures. Interestingly, the pattern of functional categories between $Hsp78_{TR}$ at 25 °C and WT at 42 °C was quite similar, suggesting that the mutations did not substantially alter the substrate range of the chaperone. The high amounts of Hsp78-interacting proteins belonging to the clusters 'energy metabolism' and 'chaperones' likely represent functional clusters of chaperone substrate proteins that are important for the maintenance of key metabolic functions of mitochondria.

Up to 70% of the total protein abundance in the different copurification samples was composed by a few individual polypeptides, most likely representing the main substrate polypeptides of Hsp78. For Hsp78 at 25 °C, these included the proteins Ilv2 (17%), Ilv1 (13%), and Alt1 (8%), all enzymes involved in amino acid biosynthesis, as well as Prx1 (9%), Mcr1 (9%), both redox homeostasis, while 50% of the signal was generated by a mixture of less abundant proteins. Switching to 42 °C, the matrix chaperone Ssc1 became predominant with almost 50% of the total signal intensity. Moreover Kgd2 (14%), Aco1 (9%), Gut2 (6%), and Sdh2 (5%), all metabolic key enzymes, were very abundant and the remaining 18% consisted of a mixture of proteins. Under recovery conditions, the amount of Ssc1 decreased again to 8%, while the abundant metabolic enzyme Ald4 (30%; aldehyde dehydrogenase) became more abundant together with Alt1 (17%), Fum1 (9%; TCA cycle), and Gut2 (6%). The intensity of other proteins increased to 29%. For $Hsp78_{TR}$, the Hsp70-chaperone Ssc1 represented the most abundant interactor with 59% already at 25 °C, while Mcr1, Prx1, Lpd1 (a major component of the pyruvate dehydrogenase complex), and Sdh2 were found with around 5% each. At elevated temperatures, the aminolevulinate synthase Hem1 (32%), Lsc2 (21%, TCA cycle), Prx1 (9%), Por1 (9%, an abundant outer membrane protein), and Ilv5 (5%, AA biosynthesis) became more abundant, while Ssc1 was strongly decreased. During recovery, Alt1 (17%) and Ald4 (17%) were the most abundant interaction partners (similar to WT), followed by Lpd1 (16%), and the chaperones Ssc1 (9%) and Hsp60 (5%) were the most abundant hits (Fig. 3*C*).

In order to visualize the behavior of the protein population and its Hsp78-binding tendency as a whole, $\log_2$ values of the quotients between sample *versus* background protein abundances were plotted for the different conditions. For individual proteins, a ratio of 1 ($\log_2$ of 0) and above implies an enrichment of the proteins by the copurification and hence binding to Hsp78. By plotting this cofractionation enrichment ratios at 25 °C *versus* those at 42 °C, we additionally visualized the role of an Hsp78-client interaction during the transition from normal to stressed conditions. As expected for a chaperone, with Hsp78, the majority of interacting polypeptides increased during heat stress. As in this visualization, the absolute amount of bound proteins was not relevant; this approach also identified low-abundance proteins that exhibited a strong interaction with Hsp78. For example, the uncharacterized protein YIL045w, a probable minor catalytic subunit of the succinate dehydrogenase, stood out as a major interacting polypeptide at both conditions. Most other proteins were higher enriched at 42 °C, notable examples were Aco1 (aconitase), which had been identified already repeatedly in previous publications as a heat-labile mitochondrial enzyme, and Ssq1, another Hsp70 chaperone family member. In addition, the graphical analysis demonstrated again the difference in client-binding behavior between the WT protein and the mutant version during the shift from 25 °C to 42 °C is clearly represented. At 25 °C, the mutant bound stronger to these potential substrates than the WT, as the cloud of protein dots accumulate near the horizontal axis, while the WT protein showed increased protein binding under heat stress conditions, as shown by the accumulation of client proteins on the vertical axis (Fig. 4*A*). Plotting the interaction data under heat stress *versus* recovery period, we observed a more similar behavior of both Hsp78 variants (Fig. 4*B*). Nevertheless, the mutant $Hsp78_{TR}$ revealed a strong binding of some proteins under recovery conditions that were not prominent as client polypeptides under heat-stress conditions. Examples for this group are the proteins Hem1 (5-aminolevulinate synthase), Mcr1 (NADH-cytochrome b5 reductase), and Lsc2 (subunit of the succinate-CoA ligase). It is conceivable that—depending on the individual structural properties of the respective proteins—an interaction with Hsp78 still persists even after a return to normal conditions in order to support potential refolding reactions.

We also tested the aggregation behavior of selected individual proteins by Western blot to confirm our qMS data (Fig. 4, *C* and *D*). Overall, the results confirm the qMS characterization, exhibiting a very variable interaction pattern at the different temperatures and also between the two forms of Hsp78 used. Both subunits of the ketoglutarate dehydrogenase complex (Kgd1 and Kgd2) exhibited a strong binding to Hsp78, in particular to the WT form, confirming their sensitivity of heat-induced aggregation (Fig. 4*C*). The amino acid biosynthesis enzyme Ilv2 showed a significant chaperone interaction already under normal temperatures, indicating a potential conformational instability that requires the chaperone activity of Hsp78 already under normal environmental

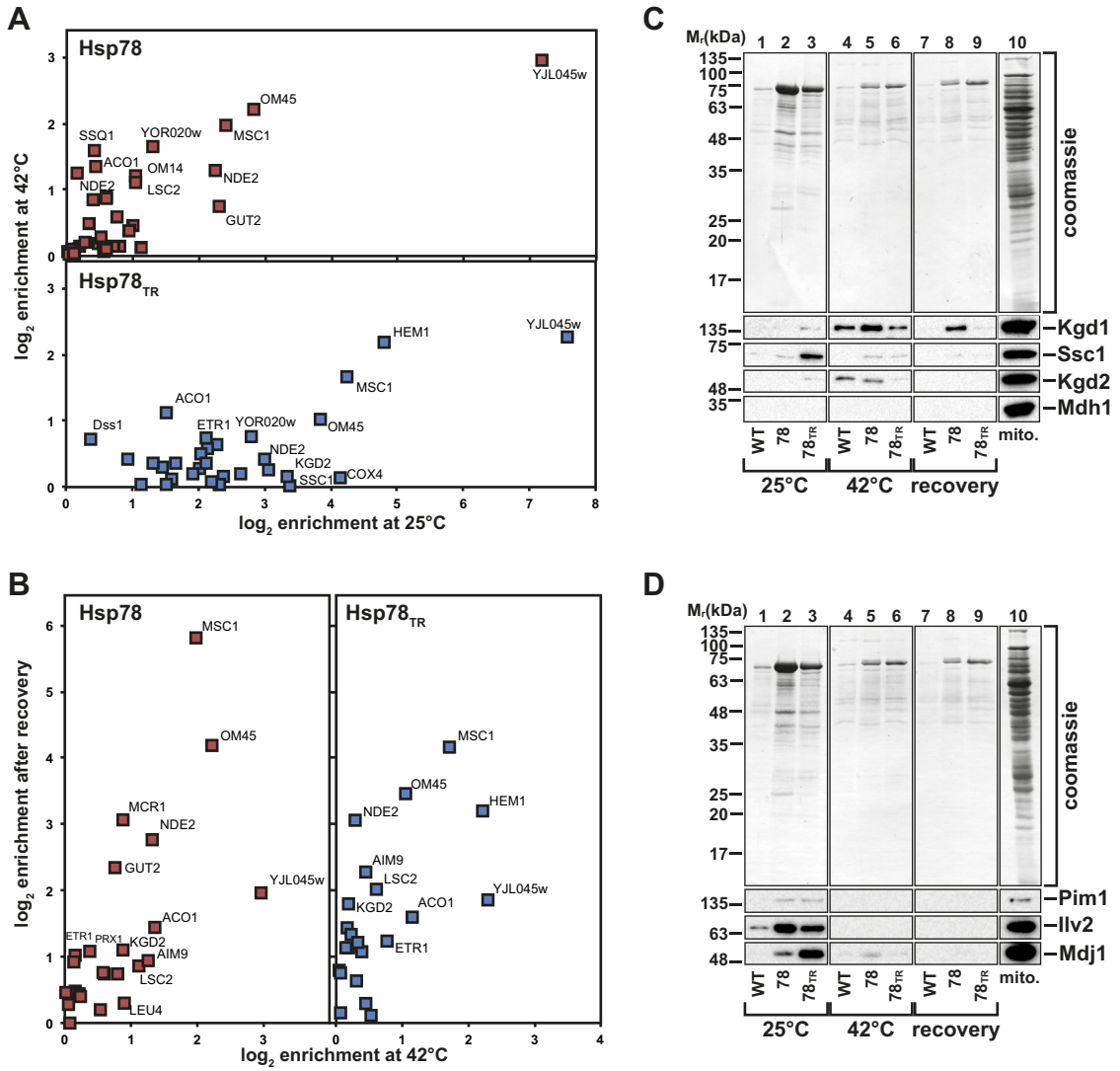

Figure 4. Copurification experiments reveal different behavior of Hsp78 and mutant Hsp78$_{TR}$ under various conditions. *A*, comparison of substrate binding at normal conditions (25 °C) and under heat stress (42 °C). Scatter plot for WT (*blue*) and mutant (*red*) Hsp78 copurification ratios over background signals (log2 values), expressing enrichment by binding affinity. Ratios are calculated from normalized average qMS abundances of three independent experiments (see Experimental procedures section; data taken from Table S3). Proteins that were detected but not enriched over background values were excluded. Strongly enriched proteins are identified. *B*, comparison of substrate binding at heat stress normal conditions (42 °C) and after 1 h recovery back at 25 °C. Data shown as described in (*A*). *C* and *D*, copurification experiment as described using WT (Hsp78) and mutant variant (Hsp78$_{TR}$) mitochondria. Eluates were analyzed by SDS-PAGE and Western blot using the indicated antisera. As loading control, the Coomassie Blue stained membrane is shown. Lane 10 (mito.) shows signals obtained with a corresponding amount of total mitochondria. qMS, quantitative mass spectroscopy.

conditions (Fig. 4*D*). The members of the mitochondrial Hsp70 system, Ssc1 and Mdj1 (the corresponding member of the DnaJ cochaperone family), showed a high interaction affinity in particular with the Hsp78$_{TR}$ mutant. The metabolic enzyme Mdh1 was served as a control for a stable soluble protein and did not copurify (Fig. 4*C*).

Identification of aggregation-prone and actively disaggregated proteins

To obtain a global overview about mitochondrial protein aggregation and disaggregation reactions, we performed an additional quantitative proteomic characterization of the general *in organello* aggregation processes, using SILAC-assisted mass spectrometry (for a workflow outline see Fig. S2). We determined protein abundances in the high-speed centrifugation pellet fractions of isolated detergent-lysed mitochondria to recover insoluble proteins as putative aggregates (prepared as described above) under different conditions. As control, mitochondria were kept at 25 °C while aggregation was induced by 30 min heat treatment at 42 °C. A potential disaggregation of polypeptides from aggregates was also assayed after a recovery incubation at 25 °C for 1 h after the heat treatment. To assess the impact of Hsp78 activity on these processes, we again used the WT and substrate-trap variants described above. We detected in total 1199 different proteins in the pellets fractions (Table S4), of which 470 were localized to mitochondria as assigned by the UniProt database, comprising on average about 96% of the total pellet protein abundance. From the 379 mitochondria-associated proteins identified at least once under every condition and in each

Hsp78 variant (Table S5), we categorized 93 (about 25%) as strongly aggregating proteins, meaning they showed a more than 4 times higher relative abundance in the pellet after 42 °C than the 25 °C pellet in mitochondria expressing Hsp78 (Fig. 5*A* and Table S5). The five most abundant proteins in the AP were Aco1, Lsc2 (both citrate cycle), Hsp60 (chaperone), Ilv5, Ilv2 (both aa biosynthesis), and Gut2 (energy metabolism). In contrast to the matrix chaperonin Hsp60, Hsp78 itself was not identified in any of the APs, indicating that it retains its solubility even during heat stress conditions, also indicating that it does not stably interact with aggregating polypeptides. The main chaperone of the matrix compartment, Ssc1 or mtHsp70, was highly abundant in the heat stress pellet fraction but also relatively strongly represented already under normal conditions and therefore barely did not meet the criteria for a strong aggregator. Of this list of strong aggregators, many were already identified above as potential Hsp78-interacting proteins, in particular the already mentioned Aco1, Lsc2, and Gut2. In addition, the identified interactors Mcr1 and Prx1 were also abundant polypeptides in the AP. Fum1, Alt1, Sdh2, and Hem1 exhibited also a high aggregation ratio.

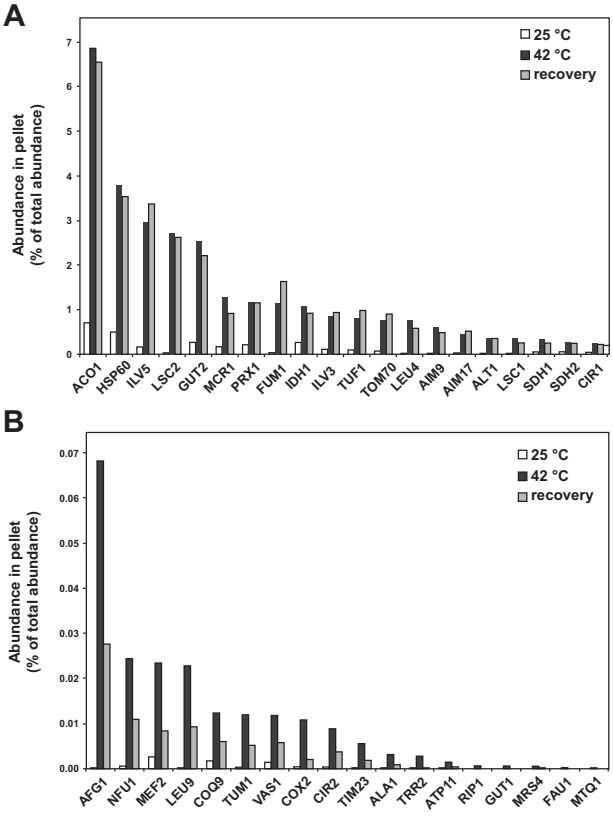

Figure 5. Identification of aggregation-prone mitochondrial proteins. *A*, relative abundance ratio in the aggregate pellets of Hsp78 and Hsp78$_{TR}$-expressing mitochondria incubated under the indicated temperature treatments (total sum of all protein abundances in the respective pellets was set to 100%). Shown are the 20 most abundant proteins in the pellets after 42 °C. Protein abundances were calculated as normalized average abundance over background from three independent experiments (see Experimental procedures section; data taken from Table S4). *B*, same dataset as in (*A*). Shown are the 20 proteins with the highest disaggregation ratio (difference between abundance after 42 °C heat stress and after 1 h recovery).

When analyzing the pellet composition after the recovery period, we observed in general no significant resolubilization of high-abundance aggregating polypeptides, suggesting that the effects of a high protein amount in the AP together with a strong aggregation propensity cannot be reversed by a disaggregation system during the reaction time of 240 min. However, some low-abundance proteins with significant aggregation propensities showed significant disaggregation (Fig. 5*B*, more than 50% reduction in the pellet), for example Afg1 (unknown function), Nfu1 (iron sulfur cluster biosynthesis), Mef2 (translation), Leu9 (aa biosynthesis), and Coq9 (ubiquinone biosynthesis). These actually disaggregating polypeptides were on average at least 10× less abundant in the AP than those that were not solubilized. Also, a few other low-abundance proteins showed a high disaggregation potential: Trr2 (redox reactions), Cox2, Atp11, Cir2 (all involved in respiration), Mrs2, Ala1, Vas1 (protein expression/translation), as well as Tim23 (protein transport) and Tum1 (sulfur metabolism). Considering a potential general negative effect of the Hsp78$_{TR}$ mutation on the aggregation reactions, we observed that the group of high-abundance aggregating proteins was barely affected, meaning the composition of the APs of Hsp78 and Hsp78$_{TR}$ was remarkably similar, both directly after the heat stress as well as after the recovery period (Fig. 6). Only a few proteins, for example, Adh4 (mitochondrial alcohol dehydrogenase), Rip1 (iron-sulfur protein of respiratory complex III), and Adk2 (GTP:AMPphosphotransferase) show significantly higher aggregation in Hsp78$_{TR}$ than in WT at 42 °C as well as after the recovery. It is therefore likely that these proteins are particularly dependent on Hsp78 activity for maintaining their solubility. However, this picture was different for the composition of the AP at 25 °C. Here, many proteins that were not strongly represented in the pellet of WT mitochondria, in particular with generally lower abundances, showed a higher aggregation rate in the Hsp78$_{TR}$ mutant (Fig. 6). This indicated that a distinct group of proteins is dependent on at least some assistance by Hsp78 to maintain their full solubility even under normal growth conditions.

For some proteins with a high aggregation tendency, including Pim1, Aco1, Ssc1, Ilv2, and Rip1, we also confirmed their aggregation behavior by a Western blot analysis. All became insoluble after 20 min of 42 °C treatment and were therefore enriched in the pellet fraction (Fig. 6, *B* and *C*). Potential clients were present with higher signal intensities in the pellet fraction of the Hsp78$_{TR}$ mutant at 25 °C, which provides further evidence to a trapping effect in the mutant. Interestingly, Rip1 showed both an increased aggregation and a decreased resolubilization rate in the mutant mitochondria, indicating an Hsp78 involvement and directly confirming the qMS results (Fig. 5*B*). The mitochondrial ribosomal complex protein Mrpl40 was expected to pellet under the chosen experimental settings and served as a positive sedimentation control (Fig. 6*B*).

Combining the results of the two proteomic approaches, we identified in total 293 proteins that were either interacting with Hsp78 or affected by aggregation/disaggregation processes in mitochondria. Criteria were either an at least two-fold

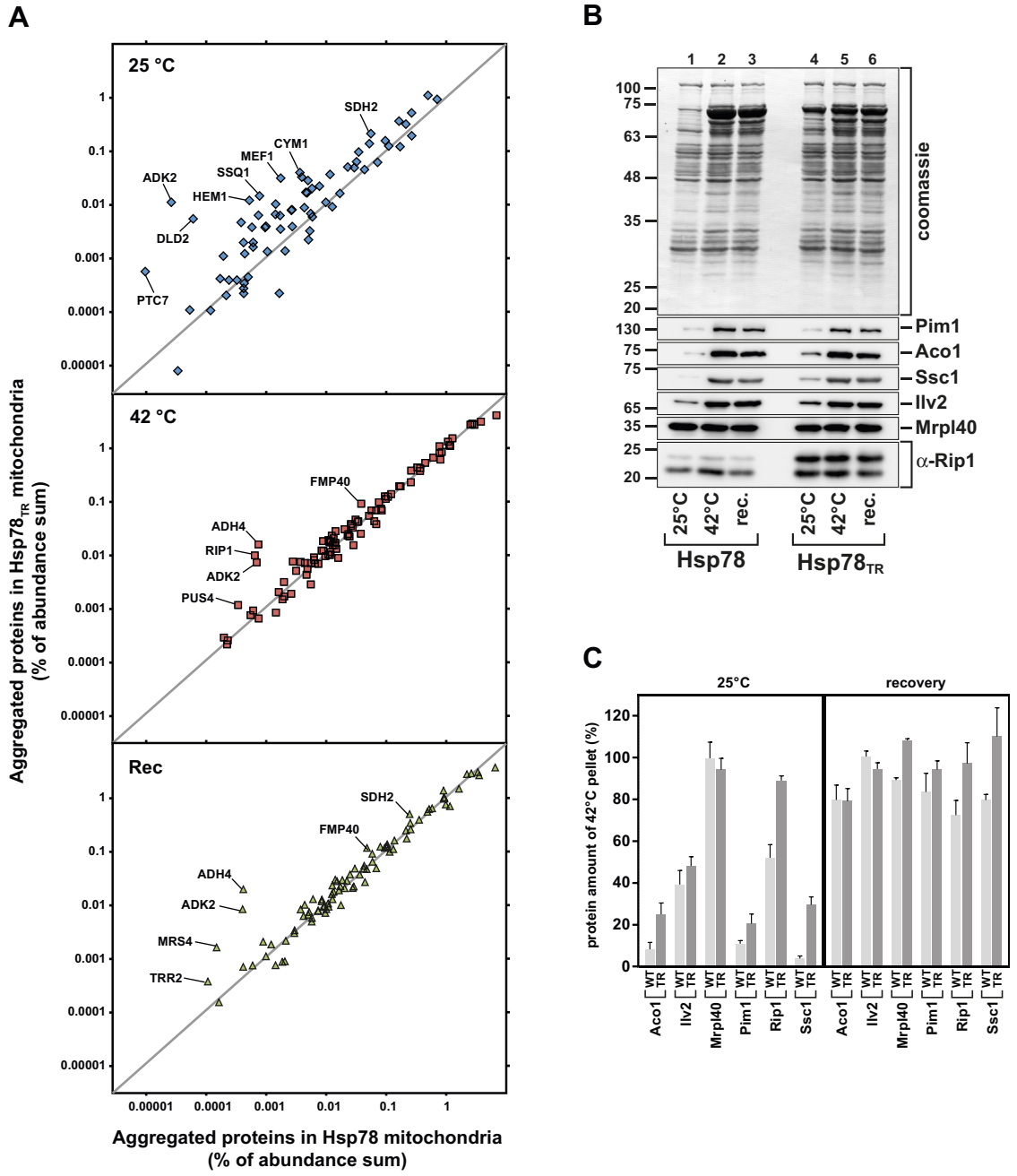

Figure 6. Proteomic aggregation and recovery assay identifies aggregation-prone proteins and reveals aggregated proteins that are resolubilized by Hsp78 function. *A*, scatter plots comparing relative abundances of proteins in aggregated pellets for WT (Hsp78) and mutant ($Hsp78_{TR}$) expressing mitochondria under the indicated temperature treatments. Dots near the diagonal represent proteins that do not differ between the two Hsp78 variants. Protein candidates with higher aggregation tendency in $Hsp78_{TR}$ are identified (data taken from Table S4). *B*, western blot analysis of aggregated pellets and control Coomassie Blue staining derived from mitochondria expressing Hsp78 or $Hsp78_{TR}$ treated with the indicated temperatures. Membranes were decorated with the indicated antisera. *C*, quantification of Western blot characterization of aggregate pellets derived from mitochondria expressing Hsp78 (WT) or $Hsp78_{TR}$ (TR) as shown in B (n = 3). Values are calculated for 25 °C and recovery conditions relative to the signal intensity at 42 °C (100%).

enrichment in the cofractionation in the pellet abundance after heat shock or a reduction in the recovery period (Fig. 7). Proteins in functional nodes represent mitochondrial translation, TCA cycle, oxidative phosphorylation, ATP synthase complex assembly, transport, amino acid biosynthesis, iron-sulfur complex binding, and chaperone-mediated protein complex assembly. Fifty-two proteins were observed in both proteome analysis approaches, representing Hsp78-dependent candidate proteins. A group of nine proteins have been identified as Hsp78-interacting polypeptides that showed significant disaggregation after heat shock, hence directly demonstrating properties for novel Hsp78 clients. All nine proteins are located in the mitochondrial matrix or at least face the matrix compartment, being accessible to Hsp78 chaperone activity. Four of these new candidates are involved in some fashion in protein synthesis at mitochondrial ribosomes (Ism1,

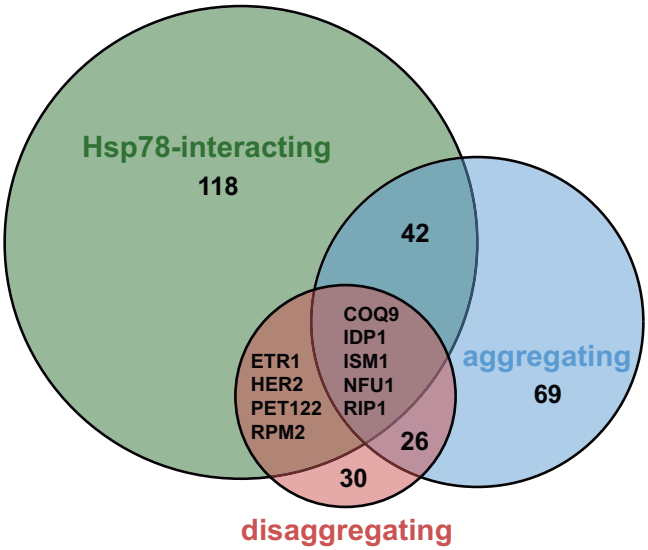

Figure 7. Venn diagram showing the distribution of identified protein hits affected by Hsp78. Shown are the numbers of mitochondrial proteins found either in the Hsp78-cofractionation analysis (*green*), sedimenting in the heat-stress aggregate pellet (*blue*), or recovering solubility after the recovery period (*red*). Only proteins enriched by at least a factor of 2 were counted (see Tables S3 and S5). *Circles* are drawn roughly to scale to indicate group sizes. Nine proteins, identified by their gene names, have been found to be disaggregating as well as directly interacting with Hsp78.

Pet122, Rpm2, and Her2) while two other in the assembly of mitochondrial Fe-S cluster, both essential mitochondrial functions.

Discussion

The chaperone Hsp78, the mitochondrial member of the Hsp100/ClpB family, has been established to play a major role in the general prevention of temperature-induced protein damage (3). However, as selected reporter proteins have been used in these studies, the full set of potential endogenous client polypeptides and the detailed role of the chaperone during mitochondrial protein aggregation are unknown so far. Hence, we performed two independent quantitative proteome analysis approaches, the first to achieve a comprehensive definition of the chaperone client spectrum under different temperature conditions and the second to characterize the role of Hsp78 function during mitochondrial protein aggregation processes. The combination of two proteomic strategies, as pursued in our study, allowed a comprehensive—and quantitative—assessment of the impact of Hsp78 on mitochondrial protein homeostasis.

The first approach utilized an affinity-based copurification of potential chaperone clients with Hsp78 as bait. As many chaperones have only a rather small affinity to their substrate proteins, we constructed a substrate-trap form of Hsp78 that carried point mutations in the Walker B motifs of the ATPase domains ($Hsp78_{TR}$). Similar setups have already been used for Hsp100 client identification in bacteria (24, 26). Similar to the corresponding ClpB mutant in *E. coli* (27), the $Hsp78_{TR}$ mutant showed a strongly reduced ATPase activity. It essentially reproduced the phenotype of an *hsp78Δ* deletion mutant, showing a strongly reduced disaggregation potential for aggregated reporter constructs (25) and a decline of acquired thermotolerance under conditions that require the metabolic activity of mitochondria (28). In line with previous published data, both Hsp78 variants assembled into higher oligomeric states favoring dimers or trimers, which in turn associated into hexameric chaperone complexes (17, 18). We found that $Hsp78_{TR}$ enzyme complexes exhibited a slightly higher stability and also in part a higher molecular weight than expected for hexamers, indicating that substrate release is reduced or delayed as the full nucleotide-dependent dynamics of the complex is required for substrate interaction and disaggregation (29). This would also be consistent with the reduced ability of $Hsp78_{TR}$ to hydrolyze ATP, which is also correlated to the dynamics of the enzyme complex (17, 18). $Hsp78_{TR}$ exhibited a slightly higher binding affinity to aggregated polypeptides *in vitro*, indicating its suitability for client identification studies. The $Hsp78_{TR}$ mutation had a direct influence on client/aggregate binding and affected strongly the overall aggregation propensity of the mitochondrial proteome. Our interaction proteome approach yielded a high number of proteins that served as new interaction and/or aggregation candidates. The large majority of hits represented mitochondrial proteins, in most cases, localized to the matrix compartment. In addition, also some inner membrane proteins with segments exposed to the matrix face were identified that may also serve as potential Hsp78 substrates. However, a few proteins from other cellular compartments, in particular ER proteins or other vesicular components, were also identified, which most likely represent postlysis-binding artefacts. These nonmitochondrial polypeptides were discounted in the data analysis.

A specific feature of our qMS analysis is the quantitative determination of the amounts of proteins found in interaction with Hsp78. For the first time, this provides information about the total substrate-flow through the chaperone system under native conditions. The total abundance sum of bound polypeptides showed a very strong increase in $Hsp78_{WT}$ under heat-shock conditions, indicating its role as a heat-stress protective chaperone. The identities of interacting proteins also strongly changed during heat shock, revealing specific substrates or partner proteins. Already at normal conditions, the absolute abundance of bound client proteins from the mitochondrial matrix was the higher for $Hsp78_{TR}$, confirming a direct and more stable substrate interaction resulting from the mutations of the Walker B motifs. Apart from that, WT and mutant Hsp78 behaved quite similar. As possible client polypeptides, we identified proteins from many different functional categories typical for mitochondrial processes. In particular, enzymes involved in energy metabolism (TCA cycle and ATP synthesis) as well as chaperone proteins were prominent Hsp78-interacting proteins, supporting the observation that Hsp78 performs an important role in the maintenance of mitochondrial functions during heat stress. As expected, the overall amount of bound polypeptides was reduced in the recovery period after the heat shock treatment but many proteins were not completely released even then.

These polypeptides probably represented clients that were still undergoing refolding or disaggregation. Interestingly, proteins from certain functional groups showed a distinct binding behavior to Hsp78 during the heat stress and the recovery period, respectively. For example, the strong interaction with components of the protein biosynthesis machinery and chaperones subsided very quickly after reduction of the temperature stress. In contrast, binding to components of the energy metabolism was largely retained even in the recovery period. This coincides with the notion that maintenance of protein biosynthesis is a primary task of the cellular stress protection system. In this line, our recent characterization of heat stress–related aggregation in mammalian mitochondria demonstrated a fast shut-off of protein translation *via* the inactivation of the translation factor TUFM (11). It is known from other studies that the mitochondrial translation together with DNA replication is strongly impaired after heat stress (23, 30, 31). Phenotypically, Hsp78 activity has been shown to be highly relevant for the stress-related recovery of intramitochondrial protein synthesis (28). The identification of components of the mitochondrial translational machinery as Hsp78 substrates is reminiscent of the formation of cytoplasmic stress granules. These dynamic structures contain RNAs and other components of the protein expression machinery and promote a rapid reactivation of protein biosynthesis after heat-stress conditions (32). The most abundant interacting polypeptides are most likely conformationally semi-stabile proteins that tend to lose their native folding state under elevated temperatures. However, not much information is available about the conformational stability of mitochondrial proteins *per se*. A potential exception is Adk2, a highly temperature-unstable matrix protein (33). Indeed, Adk2 belonged to the few proteins that also exhibited a low disaggregation efficiency and was highly dependent on Hsp78. At least, some of the identified proteins, like Kgd2, Aco1, or Ilv2, were already identified as aggregation-prone polypeptides before (34) and therefore represent major Hsp78 substrates. The main mitochondrial Hsp70-type chaperone, Ssc1, is playing a special role in this case, as it was already found to interact with Hsp78 (25). An interaction of Hsp78 with Ssc1 seems to be critical as it was shown that Hsp70s are able to stimulate the ATPase activity of Hsp100 family proteins (35). Therefore, it is likely that under heat stress conditions, Ssc1 is a functional interaction partner of Hsp78 and not only a client polypeptide itself. It is conceivable that the AAA domain mutations in $Hsp78_{TR}$ enhance this interaction with Ssc1 already under normal conditions.

Although we have previously identified a small number of aggregating mitochondrial proteins (34), we aimed our second proteomic analysis at a quantitative and more comprehensive characterization of Hsp78 influence on actual aggregation and disaggregation processes. Again, we used the impaired functionality of $Hsp78_{TR}$ as a tool to assess the impact of Hsp78 function. Comparing individual protein abundances in the AP fraction, we were able to define which proteins aggregate and were disaggregated dependent on Hsp78. In a recent proteomic characterization of yeast protein thermal stability, it was proposed that bigger and more flexible proteins may have a higher tendency for aggregation (36). Our dataset did not confirm any aggregation bias for protein size but revealed a high number of aggregation-prone proteins that exhibit specific cofactor interactions. These candidate proteins include ion binding (95 hits), nucleotide binding (60 hits), coenzyme binding (18 hits), or iron-sulfur-cluster binding (13 hits). The interaction with such cofactors, typically required for enzymatic activity, may increase the likelihood of structural instabilities, leading to an increased aggregation propensity of the affected protein. A prominent example of this category is Ilv2, which is strongly interacting with Hsp78 already under normal conditions. In its native form, it forms a large oligomeric enzyme complex containing numerous cofactor molecules (37). We were able to directly confirm the aggregation behavior of some selected proteins in biochemical experiments. This includes the chaperone Ssc1, but not its cochaperones Mge1 or Mdj1, which were previously found in aggregates (12). This might be due to the higher temperature of 48 °C and the longer heat exposition used in the former study. Moreover, we identified many proteins that were also found in a study on bacterial aggregation (bacterial homologs in brackets), such as Put2 (PutA), Kgd1 (SucA), Pda1 (AceE), Adh3 (AdhE), Aco1 (AcnB), Pim1 (Lon), Mae1 (SfcA), Sdh1 (SdhA), Lat1 (AceF), or Fum1 (FumA) among others (8), indicating an evolutionary conserved stress sensitivity of bacterial and mitochondrial proteins. We also observed a strong aggregation tendency for the yeast elongation-factor Tuf1, the homolog of the mammalian TUFM, which was found to be one of the strongest aggregating proteins in human mitochondria (11). Many of the strongly aggregating polypeptides were also found as prominent Hsp78-interacting proteins, confirming the general chaperone role of Hsp78 during aggregation processes. However, we observed that the most abundant polypeptides in the AP did not exhibit significant disaggregation rates during the recovery period. Low abundance proteins were more likely to become disaggregated, indicating that the disaggregation capacity of Hsp78, which itself is not an abundant protein, is limited to polypeptides with low expression levels. This does not exclude that also more abundant proteins may be disaggregated, but the impact on their amounts in the AP is small.

Model proteins disaggregated by Hsp78 have been shown to be directly degraded by the mitochondrial protease Pim1 (38). Indeed, many proteins prominent in our studies have been previously identified as substrates for Pim1 (39). We were able to confirm Ilv5 and Lys4 by copurification and Aco1, Ilv2, and Lsc2 by both techniques. Hence, Hsp78 and Pim1 may share a similar mechanism of substrate protein interaction, as both belong to the AAA+ protein family. Taken together, we could show that Hsp78 represents the major protein disaggregase in mitochondria during thermal stress conditions. Although it is not specialized on polypeptides from specific functional pathways, it is crucial for the recovery of mitochondria from heat-induced protein damage, rebooting processes required for functional homeostasis, like intramitochondrial protein expression energy metabolism as well as chaperone activity. It

should be noted that in addition to the action of the diverse chaperones, also other aggregation-protective processes occur in mitochondria. For instance, a recent study from our group revealed an intramitochondrial aggregation protective pathway based on the sequestration of aggregated polypeptides in inert deposition sites called IMiQ (40). Together with the enzymatic protein quality control system, this process helps to maintain general organellar integrity by relieving the chaperone system from the burden of unfolded and aggregated polypeptides (41). A future establishment of an *in vivo* aggregation and recovery assay in intact cells will be of high interest to address the balance between processes like chaperone activation, protein sequestration, and mitophagy, which all contribute to mitochondrial and cellular fitness.

Experimental procedures

Plasmids and strains

Constructs used in this study were generated by conventional cloning procedures. $Hsp78_{TR}$ mutant was generated from plasmid pTB25by site-directed mutagenesis (SDM) in two steps. First, E216Q was inserted by SDM creating plasmid pWJ01. In the second step, pWJ02 was created by SDM inserting E612Q. Subsequently, the construct was cut out by BamHI and AvrII and ligated into pTB10, resulting in a construct without histidine-tag (pWJ04). In the last step, plasmid sequence was determined and a point mutation (D386M) was recovered by SDM creating pWJ05. For tagged constructs, the mutated segment of $Hsp78_{TR}$ was cut with BamHI and AvrII and inserted into pKR09 (Hsp78-6xHis) replacing the WT segment creating pWJ07. In both pYES plasmid constructs, the encoded Hsp78 variants were under control of the galactose-inducible promotor GAL10/1. As control, expression *via* the plasmid pHSP78 was used to represent the untagged version.

All experiments were performed with *Saccharomyces cerevisae* strain Y03617-ES except in the qMS experiments, which were exclusively performed with Y13617-ES due to the use of lysine isotope forms. A list of all plasmids and strains used in this study is attached in Table S1.

Expression of Hsp78 constructs in yeast cells

Yeast cells were inoculated overnight in suitable selective growth medium containing 3% raffinose and grown at 30 °C. Cells were transferred to a medium with 3% ethanol as carbon source for respiratory growth. Expression was induced at absorbance 1 by addition of 2% galactose. Constructs were expressed for up to 4 h. For total cell extracts, cells were reisolated and dissolved in 50 µl H_20. 250 mM NaOH and 1,2% beta-mercaptoethanol was added. After an incubation for 10 min on ice, cells were TCA precipitated and 0.2 absorbance was loaded per lane for 12.5% SDS-PAGE.

In vitro *ATPase assay*

Hsp78 ATPase activity was measured by a coupled reaction for enzymatic phosphate release by PiColorLock Gold Phosphate Detection System (Novus Biologicals). For comparison, a standard curve of phosphate (0–50 µM) was measured. $Hsp78_{WT}$ and mutant $Hsp78_{TR}$ expressed and affinity purified from *E. coli* were diluted to a final concentration of 0.08 µg/µl in a volume of 500 µl reaction buffer (80 mM KCl, 10 mM $MgCl_2$, 1 mM DTT, 0.25 mM ATP, 30 mM Tris, pH 7.4). Experiments were incubated at 37 °C, and 90 µl samples were collected every 5 min up to 20 min of reaction time. Control samples were only determined after 20 min. Subsequently, enzymatic reaction Gold mix was added (1:5) to the mixture. After a short incubation of 5 min at RT, 10% of stabilizer was added and the samples were incubated for 30 min at RT according to manufacturers' directions. The resulting phosphate complex was quantified by the absorbance at 635 nm in a TECAN plate reader (96-well format).

Growth and acquired thermotolerance assays

Yeast cells were inoculated overnight in suitable selective growth medium containing 3% raffinose and grown at 30 °C. Cells were transferred to a medium with 3% ethanol as carbon source for respiratory growth. Expression was induced at absorbance 1 by sedimentation and resuspension in 2% galactose-containing medium. Cells were induced for 3 h and then heat-treated at 42 °C for 60 min in a water bath with a subsequent regeneration step for 30 min at 30 °C and a final heat exposition at 48 °C for 60 min. 10^6 cells were then diluted with water in 1:3 dilution steps and 7 µl cell suspension was spotted on selective growth plates. Plates were containing either 2% glucose for control or 3% glycerol for analysis of the mitochondrial fitness and incubated at 30 °C for several days.

Hsp78 complex formation by BN-PAGE

Intramitochondrial Hsp78 complex formation was analyzed by BN-PAGE. For that, 100 µg isolated mitochondria were incubated in buffer (250 mM sucrose, 80 mM KCl, 10 mM MOPS/KOH, pH 7.2) containing an ATP regeneration system (10 mM KPi, 10 mM creatine phosphate, 5 mM $MgCl_2$, 4 mM NADH, 3 mM ATP, 50 µg/ml creatine kinase) or buffer depleted for their nucleotide content (1 mM EDTA, 0,01 U/µl apyrase) for 10 min at RT. After reisolation, mitochondria were lysed in 100 µl ice-cold digitonin lysis buffer (50 mM KCl, 20 mM Tris–HCl, pH 7.4, 2 mM EDTA, 1 mM PMSF, 10% glycerol, 1% digitonin) by pipetting (25×). For gradient BN-PAGE (5–15%), 70 µl per lane was loaded while for SDS-PAGE control (12,5%), 30 µl was loaded. In addition, protein complex formation was also analyzed for purified Hsp78 proteins expressed in *E. coli.* To assay complex stability, 4 µg of protein was diluted in a final volume of 60 µl in protein buffer L (50 mM KCl, 30 mM Hepes, pH 7.4, 5 mM $MgCl_2$, 4 mM ATP, 2 mM EDTA, 20% glycerol) or protein buffer H (400 mM KCl, 30 mM Hepes, pH 7.4, 2 mM EDTA, 20% glycerol). After addition of 6 µl 10× BN loading dye, whole samples were used. BN-PAGE was performed according to a procedure elaborated for the analysis of multiprotein complexes from cellular lysates (42).

Aggregation and recovery assays

The [^{35}S]-radiolabeled preprotein cytb$_2$(107)-DHFR$_{DS}$, generated using the TNT T7 Quick Coupled Transcription/Translation System (Promega) was imported into isolated mitochondria for 20 min at RT, and import was stopped by the addition of 0.5 μM valinomycin. Successful and complete import was controlled by resistance of the imported polypeptides against treatment with externally added proteinase K (43). Assessment of aggregation and recovery of the imported protein were performed according to an established procedure (25) with 5 min heat stress and 60 min recovery. For the analysis of the aggregation tendency of mitochondrial proteins, isolated mitochondria were either maintained at RT, stressed for 20 min at 42 °C, or stressed and recovered for 60 to 120 min. Three times, 200 μg mitochondria from *hsp78Δ* cells were treated at 45 °C for 20 min to produce aggregates without attached Hsp78. Mitochondria were lysed by pipetting (20×) in 800 μl lysis buffer (200 mM KCl, 30 mM Tris–HCl. pH 7.4, 4 mM NADH, 3 mM ATP, 0.5 mM PMSF, 0.5% Trition X-100, protease inhibitor) each. Samples were centrifuged for 30 min at 4 °C and 125,000 × *g* to produce APs. In parallel, mitochondrial lysates were obtained from 120 μg isolated mitochondria (see above) that expressed Hsp78$_{WT}$ or Hsp78$_{TR}$ proteins. After centrifugation for 30 min at 4 °C and 125,000 × *g*, 160 μl of each cleared Hsp78 lysate corresponding to 40 μg of mitochondria was put on the *hsp78Δ* APs corresponding to an amount of 200 μg of mitochondria. Samples were incubated at 30 °C for 30 min to allow substrate binding of Hsp78. Finally, the samples were centrifuged again, and supernatant and pellet fractions were collected. While all supernatants taken were directly TCA precipitated, pellet fractions were first washed with 150 μl SEM buffer (250 mM sucrose, 10 mM MOPS, 1 mM EDTA, pH 7.2). Mock samples were added for all reactions. Protein bands were detected after SDS-PAGE by digital autoradiography and quantified by Multi Gauge software (Fujifilm) or by Western blot using specific antibodies.

Size-exclusion chromatography

Size-exclusion chromatography was performed on Äkta purifier system (Cytiva) with HiLoad 16/600 Superdex 75 column. For the run, 1 mg of Ni-NTA affinity-purified protein expressed in *E. coli* was used. Buffer GFL (50 mM KCl, 30 mM Hepes, pH 7.4, 5 mM $MgCl_2$, 2 mM ATP, 2 mM DTT, 2 mM EDTA, 20% glycerol) or buffer GFH (400 mM KCl, 30 mM Hepes, pH 7.4, 2 mM DTT, 2 mM EDTA, 20% glycerol) were used to dilute protein solution to an injection volume of 500 μl. Same buffers were used for the equilibration of the column and the run. Molecular weight markers were run only with buffer GFL. For Western blot analysis of the samples, 0.5 ml fractions were collected.

Analysis of Hsp78-interacting proteins via qMS

Yeast cells cultured in minimal medium were incubated with different isotope forms of lysine (SILAC). For cells expressing nontagged Hsp78$_{WT}$, normal lysine was used, for Hsp78$_{WT}$-6xHis $^{13}C_6$-$^{15}N_2$, L-lysine (heavy; +8), and for the mutant, Hsp78$_{TR}$-6xHis $^{2}H_4$ L-lysine (medium; +4) was added, respectively. After purification from the cells, mitochondria were treated with different temperature conditions (see above). Mitochondria (1 mg) were lysed with 2 ml lysis buffer SA (80 mM KCl, 50 mM NaP_i, pH 7.8, 5 mM $MgCl_2$, 2 mM ATP, 0.5 mM PMSF, 5% glycerol, 0.5% Triton X-100, 1× protease inhibitor) and shaking for 10 min at 4 °C. After centrifugation for 5 min at 12,000 × *g* and 4 °C, supernatants were added to 50 mg Ni-TED column material that was previously washed with lysis buffer SA. Slurry was incubated rotating at 4 °C for 15 min and applied on mini-columns. The columns were washed three times with 1 ml lysis buffer SA each and three times with 1 ml buffer SW (80 mM KCl, 50 mM NaP_i, pH 7.8, 5 mM $MgCl_2$, 2 mM ATP, 0.5 mM PMSF, 5% glycerol, 1× protease inhibitor). Finally, proteins were eluted in three fractions with 1 ml elution buffer SE (250 mM imidazole, 80 mM KCl, 50 mM NaP_i, pH 7.8, 5 mM $MgCl_2$, 2 mM ATP, 0.5 mM PMSF, 5% glycerol, 1× protease inhibitor) each. Subsequently, similar eluate volumes containing the three different Hsp78 forms were pooled and TCA precipitated and run together on a SDS-PAGE gel. For MS sample preparation, gel pieces were cut after Coomassie G-250 staining. The amount of purified bait protein served as internal loading control, while the untagged Hsp78 eluates defined the nonspecific background signals.

Analysis of mitochondrial protein aggregation and recovery qMS

For the *in organello* aggregation and recovery assay, isolated mitochondria were loaded on a multistep sucrose gradient to ensure high sample purity with low contaminations from other cellular components. The gradient was built by three layers with 4 ml 32%, 1.5 ml 23%, and 1.5 ml 15% sucrose (w/v) dissolved in EM buffer (10 mM MOPS/KOH, pH 7.2, 1 mM EDTA). Mitochondria were added on top of the gradient and covered with 1.5 ml EM buffer. After centrifugation at 125,000 × g and 4 °C for 60 min in a Beckmann SW41 Ti swinging-bucket, the mitochondria were re-extracted from the tube bottom in resuspension buffer (250 mM sucrose, 80 mM KCl, 10 mM MOPS/KOH, pH 7.2, 5 mM $MgCl_2$). Mitochondrial content was measured by Bradford assay and adjusted to a concentration of 200 μg/ml in resuspension buffer. Differently labeled mitochondria (see copurification SILAC experiment) were mixed in a 1:1 ratio using 50 μg each. Mitochondria expressing untagged Hsp78 were excluded. Samples were treated similarly to Aggregation and recovery experiments. For MS sample preparation, gel pieces were cut after SDS-PAGE.

Peptide preparation

Gel slices were subjected to tryptic in gel digestion (44). In brief, slices were washed consecutively with water, 50% and 100% acetonitrile (ACN). Proteins were reduced with 20 mM DTT in 50 mM ammonium bicarbonate and alkylated with 40 mM acrylamide (in 50 mM bicarbonate). The slices were

washed again and dehydrated with ACN. Dried slices were incubated with 250 ng sequencing grade trypsin at 37 °C overnight. The peptide extract was separated and remaining peptides extracted with 50% ACN. Peptides were dried in a vacuum concentrator and stored at -20 °C.

LC-MS measurements of peptides

Peptides were dissolved in 10 µl 0.1% formic acid (FA) and 3 µl were injected onto a C18 trap column (20 mM length, 100 µm inner diameter, ReproSil-Pur 120 C18-AQ, 5 µm; Dr Maisch GmbH, Ammerbuch-Entringen) made in-house. Bound peptides were eluted onto a C18 analytical column (200 mM length, 75 µm inner diameter, ReproSil-Pur 120 C18-AQ, 1.9 µm, with 0.1% FA as solvent A). Peptides were separated during a linear gradient from 2% to 35% solvent B (90% acetonitrile, 0.1% formic acid) within 83/90 min at 250 nl/min. The nanoHPLC was coupled online to an LTQ Orbitrap Velos mass spectrometer (Thermo Fisher Scientific). Peptide ions between 330 and 1600 m/z were scanned in the Orbitrap detector with a resolution of 60,000 (maximum fill time 400 ms, AGC target 10^6). The 22 most intense precursor ions (threshold intensity 3000, isolation width 1.2/1.0 Da) were subjected to collision induced dissociation (normalized energy 35) and analyzed in the linear ion trap. Fragmented peptide ions were excluded from repeat analysis for 20/15 s.

MS data analysis

For peptide analysis, raw data processing and database searches were performed with Proteome Discoverer software 2.1.1.21 (Thermo Fisher Scientific). Peptide identifications were done with an in-house Mascot server version 2.5.1 (Matrix Science Ltd). MS2 data were searched against *Saccharomyces cerevisiae* sequences in SwissProt (release 2017_10). Precursor ion m/z tolerance was 8 ppm, and fragment ion tolerance was 0.5 Da. Tryptic peptides with up to two missed cleavages were searched. Propionamide on cysteines was set as a static modification. Oxidation of methionine, labels $^{13}C_6{}^{15}N_2$, and $^2H_4$ on lysine were allowed as dynamic modifications. Mascot results were assigned q-values by the Percolator algorithm (45) version 2.05 as implemented in Proteome Discoverer. Spectra with identifications below 1% q-value were sent to a second round of database search with semitryptic enzyme specificity (one missed cleavage allowed) and 10 ppm MS1 mass tolerance (propionamide dynamic on Cys). In copurification experiments, only proteins were included if at least two peptides were identified with <1% false discovery rate. Typical false discovery rate values were ≤1% (peptide spectrum matches), 1.2% (peptides), and <1% (proteins). Only unique peptides were included in protein quantification.

Miscellaneous

All chemicals were analytical grade and supplied from Carl Roth if not indicated otherwise. Antisera used in this study were previously verified by band pattern comparisons of WT and respective KO strains in *S. cerevisiae*. Enzymes were purchased from Thermo Fischer Scientific. Chemicals for qMS analysis were from Sigma-Aldrich.

Further data processing

In the copurification experiments, all abundance values obtained in the control mitochondria expression nontagged Hsp78, representing nonspecific background signals, were subtracted from the respective values obtained with the tagged variants in the individual experiments and then an average value of three experiments was generated. In order to mathematically allow the calculation of copurification enrichment ratios also in cases where the respective protein has not been identified in the background control sample, abundance values were set to a minimal abundance value of 10,000, representing background intensity. All protein abundances above background were corrected by Hsp78 bait protein abundance in the respective experiment. To assess the reliability of the qMS protein identification, each protein hit was categorized concerning their identification reproducibility in isotope channels and replicate experiments. Category A proteins (best candidates) were identified with at least three peptides in all isotope channels and all experiments, category B in two replicates, and category C in one of the three replicates. Category D was not detected in any replicate of the respective temperature conditions but in others. Calculations were performed with Microsoft Excel and visualization was done using GraphPad PRISM 6. Additional protein information was collected from the UniProtKB database (https://www.uniprot.org/). Functional categories were obtained using the STRING (Protein-Protein Interaction Networks) database (https://www.string-db.org/).

Data availability

The mass spectrometry proteomics data have been deposited to the ProteomeXchange Consortium *via* the PRIDE (46) partner repository with the dataset identifiers PXD030405 (part A: protein interactions) and PXD030436 (part B: aggregation).

Supporting information—This article contains supporting information (25).

Author contributions—W. J., M. S., and W. V. conceptualization; W. J., M. S., and G. C. data curation; W. J., M. S., and W. V. formal analysis; M. S. and W. V. project administration; W. J., M. S., and W. V. resources; W. V. supervision; W. J., M. S., G. C., and W. V. validation; W. J. and W. V. writing–original draft; W. J., M. S., and W. V. writing–review and editing; W. V. funding acquisition; W. J., M. S., and G. C. investigation; W. J., G. C., and W. V. visualization.

Funding and additional information—This work was supported by the Deutsche Forschungsgemeinschaft (Grant No. VO 657/5-2 to W. V. and Projektnummer 174793735 to M. S.).

Conflict of interest—The authors declare that they have no conflict of interests with the contents of this article.

Abbreviations—The abbreviations used are: qMS, quantitative mass spectroscopy; BN, blue native; AP, aggregate pellet; SILAC, stable isotope labeling by amino acids in culture; SDM, site-directed mutagenesis; ACN, acetonitrile.

References

1. Tyedmers, J., Mogk, A., and Bukau, B. (2010) Cellular strategies for controlling protein aggregation. *Nat. Rev. Mol. Cell Biol.* **11**, 777–788
2. Voos, W. (2013) Chaperone-protease networks in mitochondrial protein homeostasis. *Biochim. Biophys. Acta.* **1833**, 388–399
3. Doyle, S. M., Genest, O., and Wickner, S. (2013) Protein rescue from aggregates by powerful molecular chaperone machines. *Nat. Rev. Mol. Cell Biol.* **14**, 617–629
4. Verghese, J., Abrams, J., Wang, Y., and Morano, K. A. (2012) Biology of the heat shock response and protein chaperones: Budding yeast (*Saccharomyces cerevisiae*) as a model system. *Microbiol. Mol. Biol. Rev.* **76**, 115–158
5. Sauer, R. T., Bolon, D. N., Burton, B. M., Burton, R. E., Flynn, J. M., Grant, R. A., *et al.* (2004) Sculpting the proteome with AAA(+) proteases and disassembly machines. *Cell* **119**, 9–18
6. Hodson, S., Marshall, J. J., and Burston, S. G. (2012) Mapping the road to recovery: The ClpB/hsp104 molecular chaperone. *J. Struct. Biol.* **179**, 161–171
7. Mogk, A., Kummer, E., and Bukau, B. (2015) Cooperation of Hsp70 and Hsp100 chaperone machines in protein disaggregation. *Front. Mol. Biosci.* **2**, 22
8. Mogk, A., Tomoyasu, T., Goloubinoff, P., Rüdiger, S., Roder, D., Langen, H., *et al.* (1999) Identification of thermolabile *Escherichia coli* proteins: Prevention and reversion of aggregation by DnaK and ClpB. *EMBO J.* **18**, 6934–6949
9. Kirstein, J., Molière, N., Dougan, D. A., and Turgay, K. (2009) Adapting the machine: Adaptor proteins for Hsp100/Clp and AAA+ proteases. *Nat. Rev. Microbiol.* **7**, 589–599
10. Chrétien, D., Bénit, P., Ha, H. H., Keipert, S., El-Khoury, R., Chang, Y. T., *et al.* (2018) Mitochondria are physiologically maintained at close to 50 °C. *PLoS Biol.* **16**, e2003992
11. Wilkening, A., Rub, C., Sylvester, M., and Voos, W. (2018) Analysis of heat-induced protein aggregation in human mitochondria. *J. Biol. Chem.* **293**, 11537–11552
12. Lewandowska, A., Gierszewska, M., Marszalek, J., and Liberek, K. (2006) Hsp78 chaperone functions in restoration of mitochondrial network following heat stress. *Biochim. Biophys. Acta.* **1763**, 141–151
13. Sanchez, Y., Taulien, J., Borkovich, K. A., and Lindquist, S. (1992) Hsp104 is required for tolerance to many forms of stress. *EMBO J.* **11**, 2357–2364
14. Leonhardt, S. A., Fearon, K., Danese, P. N., and Mason, T. L. (1993) *HSP78* encodes a yeast mitochondrial heat shock protein in the Clp family of ATP-dependent proteases. *Mol. Cell. Biol.* **13**, 6304–6313
15. Erives, A. J., and Fassler, J. S. (2015) Metabolic and chaperone gene loss marks the origin of animals: Evidence for Hsp104 and Hsp78 chaperones sharing mitochondrial enzymes as clients. *PLoS One* **10**, e0117192
16. Iosefson, O., Sharon, S., Goloubinoff, P., and Azem, A. (2012) Reactivation of protein aggregates by mortalin and Tid1–the human mitochondrial Hsp70 chaperone system. *Cell Stress Chaperones* **17**, 57–66
17. Leidhold, C., Janowsky, B. V., Becker, D., Bender, T., and Voos, W. (2006) Structure and function of Hsp78, the mitochondrial ClpB homolog. *J. Struct. Biol.* **156**, 149–164
18. Krzewska, J., Konopa, G., and Liberek, K. (2001) Importance of two ATP-binding sites for oligomerization, ATPase activity and chaperone function of mitochondrial Hsp78 protein. *J. Mol. Biol.* **314**, 901–910
19. Deville, C., Carroni, M., Franke, K. B., Topf, M., Bukau, B., Mogk, A., *et al.* (2017) Structural pathway of regulated substrate transfer and threading through an Hsp100 disaggregase. *Sci. Adv.* **3**, e1701726
20. Walker, J. E., Saraste, M., Runswick, M. J., and Gay, N. J. (1982) Distantly related sequences in the alpha- and beta-subunits of ATP synthase, myosin, kinases and other ATP-requiring enzymes and a common nucleotide binding fold. *EMBO J.* **1**, 945–951
21. Seyffer, F., Kummer, E., Oguchi, Y., Winkler, J., Kumar, M., Zahn, R., *et al.* (2012) Hsp70 proteins bind Hsp100 regulatory M domains to activate AAA+ disaggregase at aggregate surfaces. *Nat. Struct. Mol. Biol.* **19**, 1347–1355
22. Barnett, M. E., Nagy, M., Kedzierska, S., and Zolkiewski, M. (2005) The amino-terminal domain of ClpB supports binding to strongly aggregated proteins. *J. Biol. Chem.* **280**, 34940–34945
23. Wallace, E. W., Kear-Scott, J. L., Pilipenko, E. V., Schwartz, M. H., Laskowski, P. R., Rojek, A. E., *et al.* (2015) Reversible, specific, active aggregates of endogenous proteins assemble upon heat stress. *Cell* **162**, 1286–1298
24. Weibezahn, J., Schlieker, C., Bukau, B., and Mogk, A. (2003) Characterization of a trap mutant of the AAA+ chaperone ClpB. *J. Biol. Chem.* **278**, 32608–32617
25. von Janowsky, B., Major, T., Knapp, K., and Voos, W. (2006) The disaggregation activity of the mitochondrial ClpB homolog Hsp78 maintains Hsp70 function during heat stress. *J. Mol. Biol.* **357**, 793–807
26. Krajewska, J., Arent, Z., Zolkiewski, M., and Kedzierska-Mieszkowska, S. (2018) Isolation and identification of putative protein substrates of the AAA+ molecular chaperone ClpB from the pathogenic spirochaete *Leptospira interrogans*. *Int. J. Mol. Sci.* **19**, 1234
27. Mogk, A., Schlieker, C., Strub, C., Rist, W., Weibezahn, J., and Bukau, B. (2003) Roles of individual domains and conserved motifs of the AAA+ chaperone ClpB in oligomerization, ATP hydrolysis, and chaperone activity. *J. Biol. Chem.* **278**, 17615–17624
28. Schmitt, M., Neupert, W., and Langer, T. (1996) The molecular chaperone Hsp78 confers compartment-specific thermotolerance to mitochondria. *J. Cell Biol.* **134**, 1375–1386
29. Haslberger, T., Zdanowicz, A., Brand, I., Kirstein, J., Turgay, K., Mogk, A., *et al.* (2008) Protein disaggregation by the AAA+ chaperone ClpB involves partial threading of looped polypeptide segments. *Nat. Struct. Mol. Biol.* **15**, 641–650
30. Duchniewicz, M., Germaniuk, A., Westermann, B., Neupert, W., Schwarz, E., and Marszalek, J. (1999) Dual role of the mitochondrial chaperone Mdj1p in inheritance of mitochondrial DNA in yeast. *Mol. Cell. Biol.* **19**, 8201–8210
31. Shalgi, R., Hurt, J. A., Krykbaeva, I., Taipale, M., Lindquist, S., and Burge, C. B. (2013) Widespread regulation of translation by elongation pausing in heat shock. *Mol. Cell* **49**, 439–452
32. Ivanov, P., Kedersha, N., and Anderson, P. (2019) Stress granules and processing bodies in translational control. *Cold Spring Harb. Perspect. Biol.* **11**, a032813
33. Gu, Y., Gordon, D. M., Amutha, B., and Pain, D. (2005) A GTP:AMP phosphotransferase, Adk2p, in *Saccharomyces cerevisiae*. Role of the C terminus in protein folding/stabilization, thermal tolerance, and enzymatic activity. *J. Biol. Chem.* **280**, 18604–18609
34. Bender, T., Lewrenz, I., Franken, S., Baitzel, C., and Voos, W. (2011) Mitochondrial enzymes are protected from stress-induced aggregation by mitochondrial chaperones and the Pim1/LON protease. *Mol. Biol. Cell* **22**, 541–554
35. Lee, J., Kim, J. H., Biter, A. B., Sielaff, B., Lee, S., and Tsai, F. T. (2013) Heat shock protein (Hsp) 70 is an activator of the Hsp104 motor. *Proc. Natl. Acad. Sci. U. S. A.* **110**, 8513–8518
36. Leuenberger, P., Ganscha, S., Kahraman, A., Cappelletti, V., Boersema, P. J., von Mering, C., *et al.* (2017) Cell-wide analysis of protein thermal unfolding reveals determinants of thermostability. *Science* **355**. eaai7825
37. Lonhienne, T., Low, Y. S., Croll, T., Gao, Y., Wang, Q., Garcia, M. D., *et al.* (2020) Structures of fungal and plant acetohydroxyacid synthases. *Nature* **586**, 317–321
38. Röttgers, K., Zufall, N., Guiard, B., and Voos, W. (2002) The ClpB homolog Hsp78 is required for the efficient degradation of proteins in the mitochondrial matrix. *J. Biol. Chem.* **277**, 45829–45837
39. Major, T., von Janowsky, B., Ruppert, T., Mogk, A., and Voos, W. (2006) Proteomic analysis of mitochondrial protein turnover: Identification of novel substrate proteins of the matrix protease Pim1. *Mol. Cell. Biol.* **26**, 762–776

40. Bruderek, M., Jaworek, W., Wilkening, A., Rüb, C., Cenini, G., Förtsch, A., *et al.* (2018) IMiQ: A novel protein quality control compartment protecting mitochondrial functional integrity. *Mol. Biol. Cell* **29**, 256–269
41. Sontag, E. M., Samant, R. S., and Frydman, J. (2017) Mechanisms and functions of spatial protein quality control. *Annu. Rev. Biochem.* **86**, 97–122
42. Fiala, G. J., Schamel, W. W., and Blumenthal, B. (2011) Blue native polyacrylamide gel electrophoresis (BN-PAGE) for analysis of multiprotein complexes from cellular lysates. *J. Vis. Exp.* **48**, e2164
43. Lim, J. H., Martin, F., Guiard, B., Pfanner, N., and Voos, W. (2001) The mitochondrial Hsp70-dependent import system actively unfolds preproteins and shortens the lag phase of translocation. *EMBO J.* **20**, 941–950
44. Rosenfeld, J., Capdevielle, J., Guillemot, J. C., and Ferrara, P. (1992) In-gel digestion of proteins for internal sequence analysis after one- or two-dimensional gel electrophoresis. *Anal. Biochem.* **203**, 173–179
45. Käll, L., Storey, J. D., MacCoss, M. J., and Noble, W. S. (2008) Assigning significance to peptides identified by tandem mass spectrometry using decoy databases. *J. .Proteome Res.* **7**, 29–34
46. Perez-Riverol, Y., Csordas, A., Bai, J., Bernal-Llinares, M., Hewapathirana, S., Kundu, D. J., *et al.* (2019) The PRIDE database and related tools and resources in 2019: Improving support for quantification data. *Nucleic Acids Res.* **47**, D442–D450